



ELSEVIER

Contents lists available at ScienceDirect

## Organic Electronics

journal homepage: [www.elsevier.com/locate/orgel](http://www.elsevier.com/locate/orgel)

## Letter

# Microwires and microtwists from X-shaped conjugated molecules as low-loss, long distance photo waveguide materials

Ting Lei<sup>a</sup>, Hai-Bo Chen<sup>a</sup>, Jie Yin<sup>a</sup>, Shan Huang<sup>b</sup>, Xing Zhu<sup>b,\*</sup>, Jian Pei<sup>a,\*</sup>

<sup>a</sup>The Key Laboratory of Bioorganic Chemistry and Molecular Engineering and of Ministry of Education, College of Chemistry and Molecular Engineering, Peking University, Beijing 100871, China

<sup>b</sup>The State Key Laboratory for Mesoscopic Physics, School of Physics, Peking University, Beijing 100871, China

## ARTICLE INFO

## Article history:

Received 6 October 2010

Received in revised form 25 December 2010

Accepted 27 December 2010

Available online 8 January 2011

## Keywords:

Microwires

Chiral structure

Conjugated molecules

Photo waveguide

Solution process

## ABSTRACT

Single crystalline microwires and polycrystalline microtwists were self-assembled from X-shaped conjugated molecules through solution process in high yield. The excellent long-range optical waveguide ability and efficient light transfer between wires made the as-prepared microwires potential building blocks for complex optical devices at micrometer scale. By slight structural change, well-dispersed polycrystalline microtwists were also successfully obtained. We further demonstrated that such chiral structures could also be used as optical waveguiding materials. The investigation of photo waveguide property in the well-dispersed single microtwist is the first demonstration of chiral microstructures in the application of optical waveguide, which opens the possibility of coupling the chirality of material to that of light.

© 2011 Elsevier B.V. All rights reserved.

## 1. Introduction

Due to the quantum effects of electrons, traditional integrated circuits are facing serious challenges when the device size goes down to tens of nanometers. Therefore, it is important to exploit novel optical materials and technologies for information transmission and processing in the next generation information and communication systems. Most recently, considerable attention has been paid to the preparation and fabrication of semiconducting nanomaterials due to their potential applications as active materials in miniaturized optoelectronic devices [1–8]. Among all kinds of functional optoelectronic materials, submicrometer photo waveguide materials play an important role in integrated light-based devices [9–11]. They can be used to control the efficient delivery of light at nano or micrometer scale, indicating the possibility of high-speed and low-loss integrated circuit. One dimensional single

crystal inorganic nanowires for active photo waveguide materials have been obtained through chemical vapor deposition (CVD) or physical vapor deposition (PVD) method, and their photo waveguide properties, including the optical cavity effect and lasing, have been extensively studied [12–16]. Very recently, nano- or micro- architectures (mostly 1D structures) self-assembled from conjugated organic molecules through solution process have been attracting increased interest in this field [3–8]. They might serve as better media to generate or propagate light in a predefined way, due to their flexibility, easy optical tunability, strong luminescence efficiency [17–30]. However, waveguiding behavior has been observed only in few organic materials. Hence, the challenge of fabricating organic nanowires, which could provide photo waveguide devices with enhanced performance and more functionality, is a subject of significant scientific interest and technological importance.

Herein, we report the photo waveguiding behaviors of single crystalline microwires and polycrystalline microtwists fabricated by solution process from a new kind of X-shaped  $\pi$ -conjugated molecules synthesized by us recently [31]. These ultralong microstructures provide us

\* Corresponding authors. Tel.: +86 10 6275 8145; fax: +86 10 6275 1708.

E-mail addresses: [zhuxing@pku.edu.cn](mailto:zhuxing@pku.edu.cn) (X. Zhu), [jianpei@pku.edu.cn](mailto:jianpei@pku.edu.cn) (J. Pei).

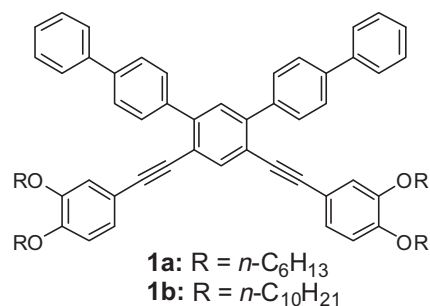
much convenience in the fabrication of optical and electronic devices. Fluorescence microscope and scanning near-field optical microscope (SNOM) show that our 1D microstructures can serve as long-distance active optical waveguides, which allow locally excited photoluminescence to propagate along the 1D structure and out-couple at the tip. We further observed excellent coupling between the as-synthesized organic wires, which is an important element in the construction of complex optical circuits. The ability to change the direction of light would be of great interest for real application in miniaturized complex photonic devices [9–11]. By slight change in chemical structure, we have obtained well-dispersed single microtwist and further demonstrated that such chiral structures could also be used as optical waveguiding materials. Our microtwist is the first chiral structure for waveguide research and opens the possibility of coupling the chirality of material to that of light.

## 2. Materials and methods

X-shaped molecules were synthesized in our recently published paper [31]. Absorption spectra were recorded on PerkinElmer Lambda 35 UV–vis Spectrometer. Photoluminescent (PL) spectra were carried out on PerkinElmer LS55 Luminescence Spectrometer. Thermal gravity analyses (TGA) were carried out on a TA Instrument Q600 analyzer and differential scanning calorimetry (DSC) analyses were performed on a METTLER TOLEDO Instrument DSC822e calorimeter. Scanning electron microscopy (SEM) was performed on a Philips XL30W/TMP operating at 1 kV. Transmission electron micrographs (TEM) were recorded on a Philips model Tecnai F20 electron microscope operating at 120 kV. Powder X-ray diffraction was recorded on a D/max-RA High Power Rotating Anode 12KW X-ray Diffractometer. Refractive index was measured on a HORIBA JOBIN YVON spectroscopic ellipsometer. The fluorescence images were taken on a DMLS fluorescence microscope (Leica, Germany). The optical waveguide properties were measured with a scanning near-field optical microscope composed of a NSOM-100 near field scanning tip (Nanonics Co.), SPM-100 (RHK Co.) controller and SPEX 0.34 fluorescence optical spectrometer.

## 3. Results and discussion

Scheme 1 illustrates the chemical structure of our X-shaped molecules. Fig. 1 shows the absorption and photoluminescence (PL) spectra of **1a** in  $\text{CH}_2\text{Cl}_2$  solution and in the crystalline state. The monomer exhibits two resolved absorption peaks at 300 and 327 nm, and a relative weak shoulder peak at about 350 nm. All absorption peaks slightly red-shifted after the molecules self-assembled into microwires, and the intensity of the shoulder peak increases considerably. In the dissolved state, **1a** exhibits a single emission peak at about 414 nm. In the solid state, a small red-shift of the photoluminescence peak was observed. The small red-shifts in absorption and fluorescence spectra on going from solution to solid state indicated that the  $\pi$ – $\pi$  stacking interactions among the molecules are not



Scheme 1. Chemical structure of X-shaped molecule **1a** and **1b**.

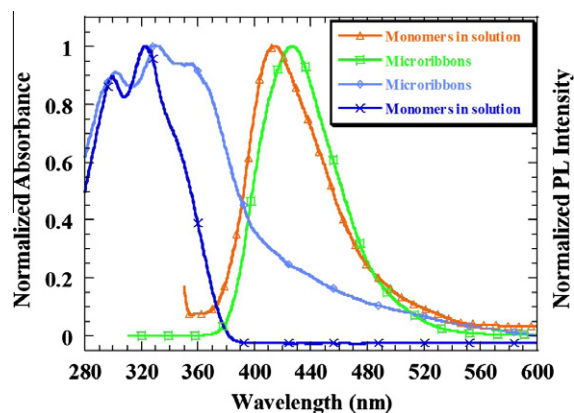
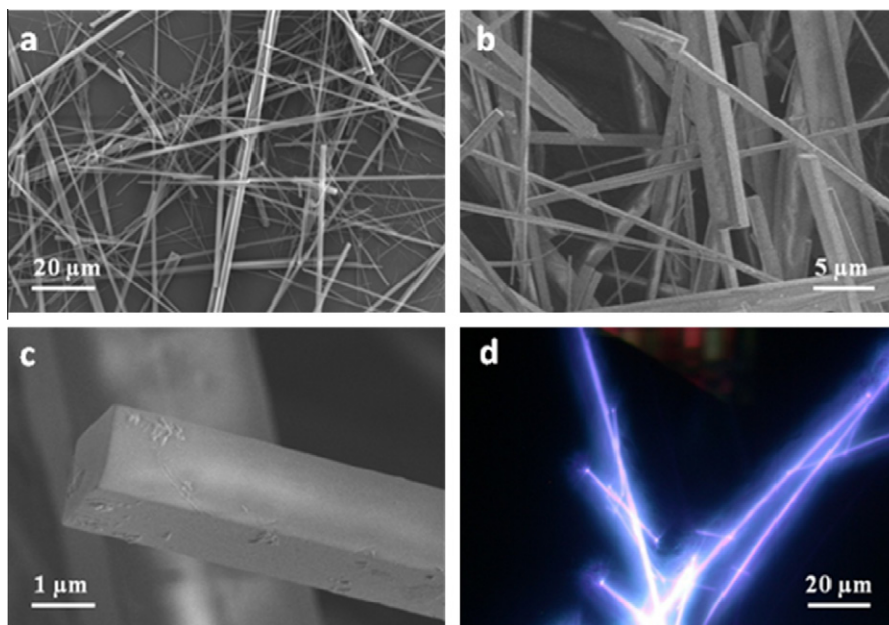


Fig. 1. Normalized absorption and emission spectrum of **1a** in dilute  $\text{CH}_2\text{Cl}_2$  solution ( $1 \times 10^{-6}$  M) and in single-crystalline microribbons.

very strong in the microwires. The photophysical properties of **1b** are almost the same as that of **1a** due to the same skeleton.

A facile method that combines reprecipitation and self-assembly techniques [5] was developed to fabricate the single-crystalline microribbons. Experimentally, the microstructures were prepared by dissolving the molecule **1a** in mixed solvents of  $\text{CH}_2\text{Cl}_2$  and EtOH (1:1.5, V/V) at a concentration of 1 mg/mL and stay with slow evaporation of the solvents. The slow crystallization process results in the formation of ribbon-shaped aggregates from the self-assembly of the molecules. Fig. 2 shows typical scanning electron microscopy (SEM) and fluorescence microscope images of the microribbons. Large-area SEM images of an EtOH suspension of self-assembled **1a** through slow crystallization process on silica substrate showed a uniform fibrous structure (Fig. 2a). Most of the microribbons are hundreds of micrometers long and 1–4  $\mu\text{m}$  wide. Small area SEM image (Fig. 2b) demonstrated that each single ribbon has a fixed size along its entire length. The cross-sections of the microribbons are rectangular (see Fig. 2c), which is a propitious condition to realize the fluorescence out-coupling at the end of the ribbons compared with the microstructures with irregular tips. Some thinner nanowires with length of tens of micrometers and width of 200–400 nm were also found. The selected area electron diffraction (SAED) pattern indicated that the



**Fig. 2.** Morphologies of the microribbons. (a) Large-area; (b) small-area and (c) further amplified SEM image of single-crystalline microribbons prepared from **1a** (1 mg/mL). (d) Photoluminescence images of the microribbons.

ribbon-shaped 1D morphology was single crystalline [31]. Fig. 2d shows a PL microscopy image of the microribbons on glass substrate. The microribbons were transferred onto the substrate by spin casting and were directly observed by using a PL microscope. The PL image shown in Fig. 2d indicates that the microribbons exhibit blue emission, with very bright luminescence spots at both tips and relatively weaker emission from the bodies of the ribbons. This is a typical characteristic of an optical waveguide material.

Photoluminescence images of the microribbons on a glass substrate reveal that they are suitable for long-range optical waveguide materials. To study the detailed waveguiding properties of the microribbons, we employed a continuous laser focused down to the diffraction limit ( $\sim 5 \mu\text{m}$ ) with a wavelength of 325 nm according to the absorption spectrum of the microribbon. The local emission of light from each single microribbon under laser excitation was so strong that it could be imaged clearly with a color CCD. Fig. 3a shows the micro area fluorescence microscopy image of a single microribbon obtained from scanning near-field optical microscopy (SNOM) in bright field, indicating that the ribbons are suitable single wire long range photo waveguide materials. Guided PL was emitted from both ends of the microribbons irrespective of the excited position. No emission was detected other than the tips and the excited area. It can be supposed that due to a large enough diameter of the crystallite (larger than excitation and fluorescence wavelength), luminescence excited on the ribbon surface spreads out inside the ribbon by means of total internal reflection [22].

A SNOM collection tip was placed stationary at one of the ribbon ends to detect the out-coupled fluorescence. As shown in Fig. 3b, the PL spectra collected at different transmitted distance are very similar, with only a slight

red-shift due to self-absorption at low wavelength. The process of light traveling along the wire can be investigated by moving the laser along the ribbon, as shown in Fig. 4. The distance-dependent photoluminescence spectra, showing propagation of light through single microribbons, were also measured with a SNOM. The PL intensity at 424 nm decreases with increasing the guided distance, without any change in outcoupled position (Fig. 3c). The optical loss mainly comes from the reabsorption during propagation of light and coupling between the ribbons and the substrates. Another possible source for the optical loss is the Rayleigh scattering arising from defects and roughness, which will result in the local variation in the refractive index along the length of the ribbons.

$$\alpha = -10 \times \log(I_{\text{out}}/I_{\text{in}}) \times L^{-1} \quad (1)$$

The optical loss coefficient of guided fluorescence in the microribbons can be calculated by the following Eq. (1).  $I_{\text{out}}$  and  $I_{\text{in}}$  are the intensities of incidence and out-coupled light, and  $L$  is the propagation distance [30]. The loss coefficients at 424 nm in the microribbons is determined to be 4.9 dB/100  $\mu\text{m}$ , which is much lower than those of many 1D organic nanomaterials reported before [28–30]. This indicated that the microribbons are excellent candidate for low-loss, long-distance optical waveguide material. The PL of the microribbons at 424 nm displays linear losses (Fig. 3d) with increasing propagation length. Hence, by using the loss coefficient and the value of  $I_{\text{in}}$  from the spectrum of  $L = 40 \mu\text{m}$  in Fig. 3d, one could calculate the theoretical intensity of PL at different wavelengths guided through different distance ( $L$ ) along the microribbons.

The transition from spontaneous PL to stimulated emission is significantly influenced by the size and length of the

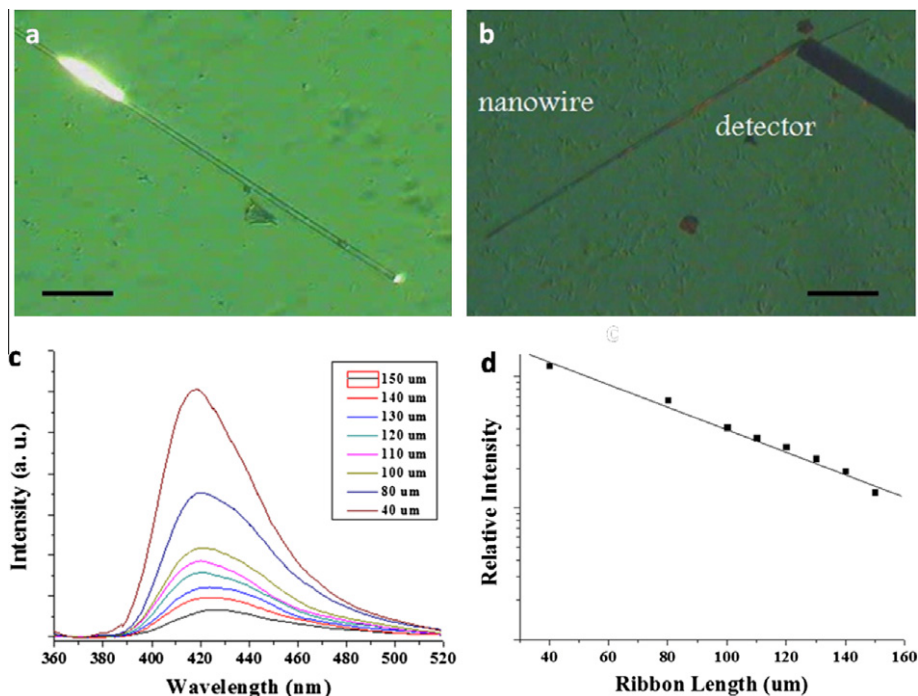


**Fig. 3.** (a) Micro area fluorescence microscopy image of an excited single microribbon in bright field. (b) The detection of the out-coupled fluorescence: a SNOM collection tip was placed stationary at one of the ribbon ends. (c) The distance-dependent photoluminescence spectra of propagated light through single microribbon measured with an SNOM detection tip. (d) The logarithmic plot of relative intensities of PL peak at 500 nm. Scale bars: (a) 20 μm, (b) 40 μm.

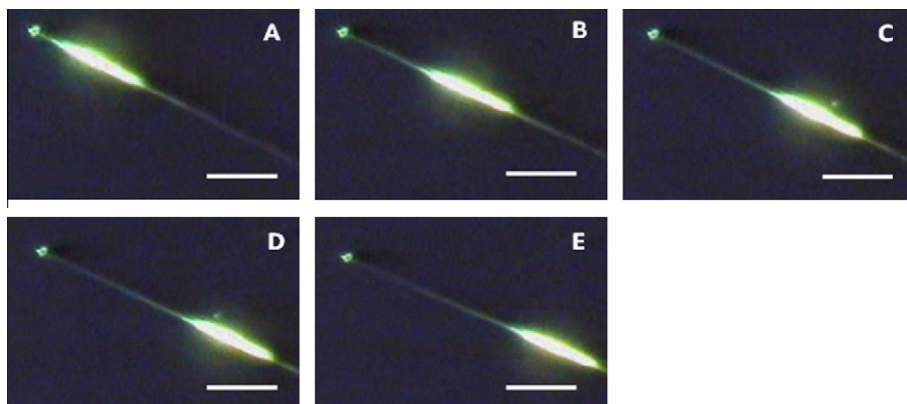


**Fig. 4.** Selected images of an excited microwire with different guided distance. (A) 40 μm; (B) 80 μm; (C) 100 μm; (D) 110 μm and (E) 120 μm.

microribbons. For example, for thinner ribbons with a width of 300–400 nm, no emission was detected at the tip of the ribbon (Fig. 5). It has been demonstrated that light can only propagate within the transverse magnetic (TM) modes of microribbon waveguides [24], whereby the number of possible modes,  $m$ , is restricted by

$$m < \frac{2a}{\lambda} \cdot \frac{n_{\perp}}{n_{\parallel}} \cdot \sqrt{n_{\parallel}^2 - n_s^2} \quad (2)$$

with  $a$  being the width of the ribbon;  $\lambda \approx 424$  nm, the wavelength of the propagated light,  $n_{\parallel}$  and  $n_{\perp}$ , the refractive indices along and perpendicular to the microribbon,

respectively, and  $n_s = 1.46$ , the refractive index of the quartz substrate. Here, we assume that both  $n_{\parallel}$  and  $n_{\perp}$  are close to the value of the bulk material ( $\approx 1.62$ ), which was measured using a spectroscopic ellipsometer (as shown in Fig. 6). According to the Eq. (2), the minimum width required for light propagation at 424 nm is approximately 302 nm as given by  $m = 1$ . This is consistent with the experimental observations that thinner ribbons with a width of 300 nm exhibit no long-range optical waveguide properties. The maximum mode ( $m$ ) that a microwire with width of 2 μm could propagate is 6.

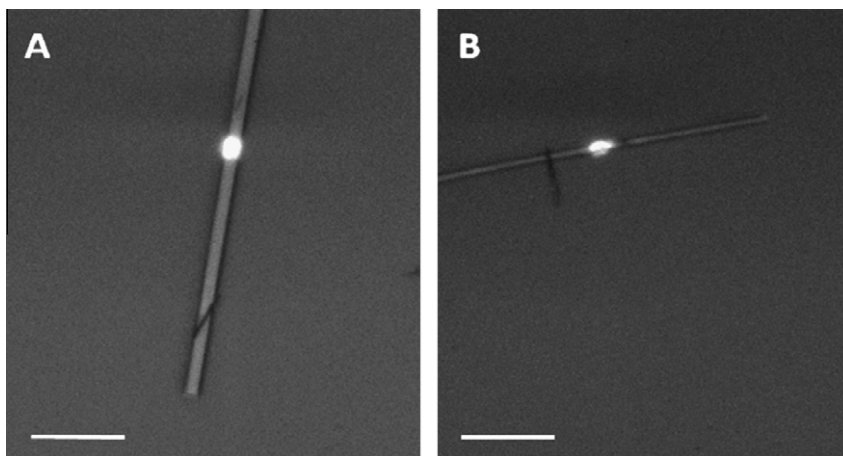


Fig. 5. SNOW image of a single wire with a width of about 300 nm: No emission was detected at the tip of the wire. Scale bars: (A) 2  $\mu\text{m}$  and (B) 5  $\mu\text{m}$ .

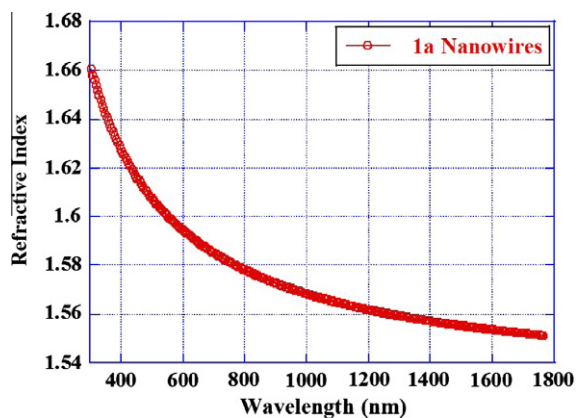


Fig. 6. The wavelength-dependent refractive index of the microwires measured with an HORIBA JOBIN YVON spectroscopic ellipsometer.

The cutoff wavelength above which no propagating mode can exist can be given as follows:

$$\lambda_{\text{cutoff}} = 2a\sqrt{n_{\parallel}^2 - n_s^2} \quad (3)$$

By using the above values of  $n_{\parallel}$ ,  $n_{\perp}$  and  $n_s$ , the  $\lambda_{\text{cutoff}}$  is calculated to be 421 and 1402 nm when  $a = 300$  and 1000 nm, respectively. This mode analysis implies that due to the cutoff effect, the ribbons with a width of about 300 nm may exhibit a significant increase in the optical loss for  $\lambda > 421$  nm. The cutoff effect can be observed only for ribbons with a relatively narrow width because  $\lambda_{\text{cutoff}}$  is out of the wavelength range of the emission band for fibers wider than 650 nm. In our case, most of the ribbons were 1–4  $\mu\text{m}$  along the 1D direction, so the cutoff effect has negligible influence on the out-coupling fluorescence at 424 nm.

Excellent coupling effect (Fig. 7) was found in the system of two or more ribbons from molecule **1a**, which was unusual in organic micrometer scale photo waveguide materials. In Fig. 7a and b, both the right ends of ribbons A and B emitted luminescence as long as any one of the left

ends was excited by the laser. This observation suggested that part of the light is transferred from one ribbon to another, and the residual light propagated along the same ribbon. Similar coupling behavior could also be observed for 3 or more microwires, as shown in Fig. 7c and d. The left end of ribbon C emitted intrinsic luminescence of the microribbon if the right end of ribbon A was excited, showing the transfer of light among three ribbons, which was never reported before. This phenomenon is common in our material. We tentatively proposed that the transfer of the light took place at the contact point of the two fibers where the difference of the refractive index disappeared. The surface condition of the fibers at the contact point is an important factor for the transfer of the light. As an example, in Fig. 7b, 46% of the light intensity transfer into ribbon A from ribbon B at the contacting point according to the known loss constant (Fig. 8). The unique feature of the microfibrers provides us a convenient way to control the direction and distribution of the fluorescence, indicating the potential in building complex optical system in micrometer or submicrometer scale.

Usually, waveguiding materials have simple geometric shapes such as wire and ribbon. We wondered whether complex microstructure could also be used to transport light and whether such materials would give new physical phenomena. As we reported recently, by simply changing the length of peripheral alkoxy groups, well-dispersed, regular microtwists were easily obtained [31]. Such a large change in morphology was remarkable. We ascribed such change to different crystal growth kinetics of **1a** and **1b**. In short, the imbalance in the growth rate between the center and the edge part of a growing front provided the driving force for twist growth in **1b** [31]. In the preparation of the manuscript, Luis Sánchez and coworkers also reported a similar system for the growing of chiral one-dimensional microstructures. However, in our system, the chirality of the microwires was not induced by the chirality of the side alkyl chains but by the intrinsic crystal packing [32]. Fig. 9a shows a SEM image of the microtwists prepared at 15  $^{\circ}\text{C}$  through solution process. The fluorescence microscope image of the microtwist on glass substrate (Fig. 9b and inset)

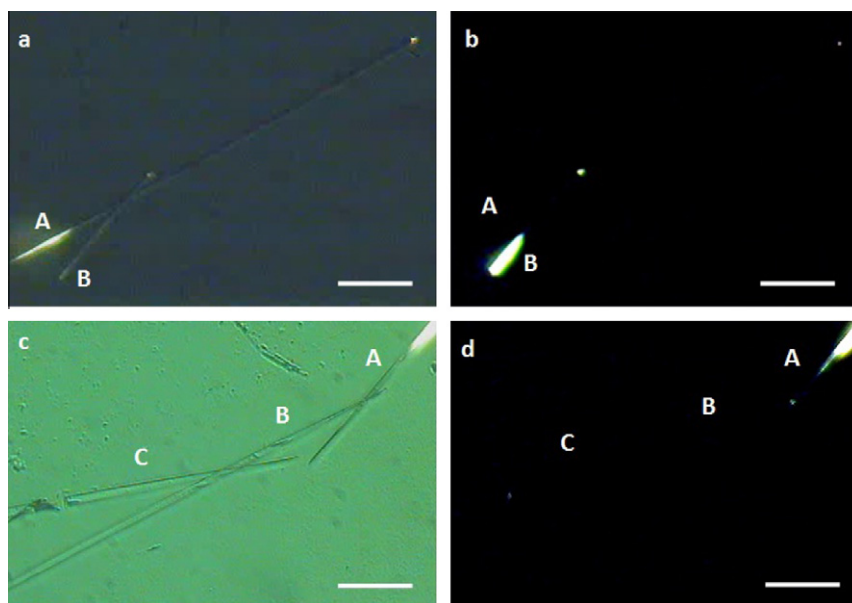


**Fig. 7.** Coupling effect in the microribbons. (a) Coupling effect in a two-ribbon system in bright field, excitation position: left end of microribbon A. (b) A corresponding picture of the two-ribbon system in dark field, excitation position: left end of microribbon B. (c) Coupling effect in a three-ribbon system in bright field, excitation position: right end of microribbon A. (d) A corresponding picture of the three-ribbon system in dark field, excitation position: right end of microribbon A. Scale bars: (a) 20  $\mu\text{m}$ , (b) 20  $\mu\text{m}$ , (c) 10  $\mu\text{m}$  and (d) 10  $\mu\text{m}$ .

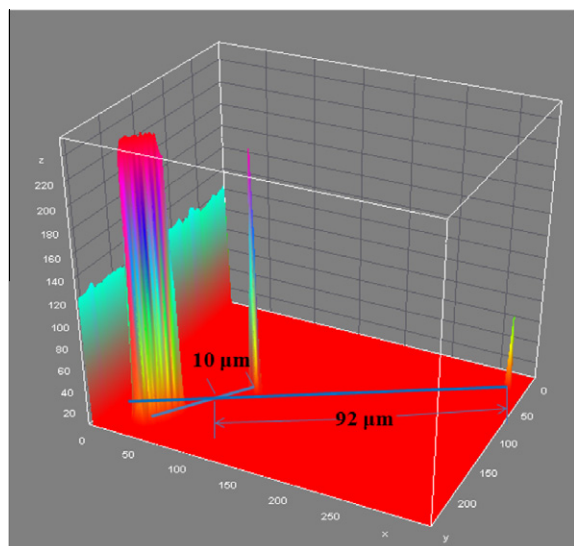


**Fig. 8.** The calculation of the transfer efficiency in Fig. 7b.

indicates that such chiral structure could also serve as optical waveguide materials. The distance-dependent photoluminescence spectra along a single microtwist were also measured with a SNOM. Fig. 9d shows the logarithmic plot of relative intensities of PL peak of the microtwists with a pitch of 1  $\mu\text{m}$ . The microtwist showed photo waveguide properties similar to that of the microwire. Although its loss coefficient is systematically higher (8.3 dB/100  $\mu\text{m}$  with a pitch of 1  $\mu\text{m}$  according to Eq. (1)), the loss coefficient is still lower than many other organic photo waveguide

materials [30]. The comparatively higher performance of the microribbons can be attributed to two factors: first, as demonstrated by SAED experiment [31], the microribbons are single crystalline while the microtwists are relative polycrystalline. Single crystalline materials are known to have superior device performance due to less grain boundaries and scattering. Second, the dramatic curvature change at the groove of the twists might constitute many scattering sites, which further increased the optical loss. The scattered strength should be strongly dependent on the size of the scattering center; further investigation is undergoing focused on these problems. In general, the loss coefficient increased with the decrease of the pitch, which is a result of the lower crystallinity and more scattering sites. Nevertheless, the ability of realizing single twist device with definite chirality allowed us to explore the interesting possibility of chirality-coupled optical devices. We are currently examining this possibility in a single left-handed or right-handed twist.

#### 4. Conclusion

In summary, we have demonstrated a series of 1D microstructure which can be used as optical waveguide materials. 1D microwires and microtwists were prepared from X-shaped conjugated molecules through simple solution process in high yield, which provides us a convenient and low-cost fabrication method for functional organic microstructures. The as-prepared microwires demonstrated excellent properties in low-loss long-distance (4.9 dB/100  $\mu\text{m}$ , >200  $\mu\text{m}$ ) photo waveguide in single wire as well as the transfer of light between the wires, showing the potential as building blocks in complex optical devices

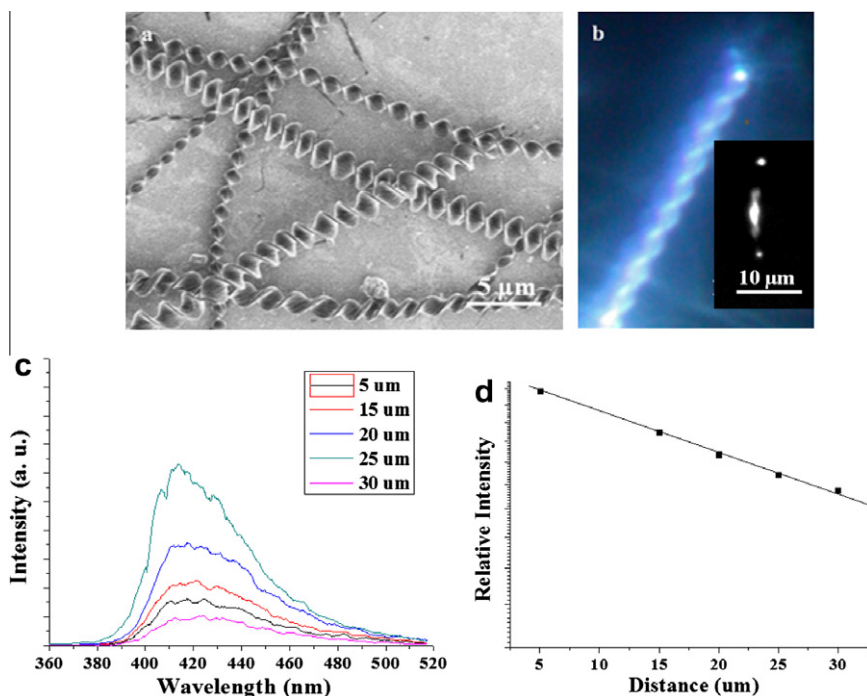


**Fig. 9.** (a) SEM image of the microtwists prepared at 15 °C. (b) Photoluminescence images of a single microtwist. Inset: the photo waveguiding behavior of the microtwist. (c) The distance-dependent photoluminescence spectra of propagated light through single microtwist measured with an SNOM detection tip. (d) The logarithmic plot of relative intensities of PL peak at 424 nm.

at micrometer scale. On the other hand, we were also able to greatly change the morphology of the microstructure by a slight change in the chemical structure. Our microtwist is the first chiral material that shows waveguiding properties. Despite the medium performance (8.3 dB/100 μm), realization of photo waveguiding in chiral materials suggest many interesting possibilities for novel devices. Further efforts would be made to control the distribution of PL between two wires, and to reveal the relationship between the coupling efficiency and the surface condition of the wires at the contact point. Also, we are further developing microtwists with pitch comparable to the wavelength of guided light in order to check whether the chirality of the materials would influence its interaction with light.

### Acknowledgments

This work was supported by the Major State Basic Research Development Program (Nos. 2006CB921602 and 2009CB623601) from the Ministry of Science and Technology and National Natural Science Foundation of China.

### References

- [1] J. Hu, T.W. Odom, C.M. Lieber, *Acc. Chem. Res.* 32 (1999) 435.
- [2] Y. Xia, P. Yang, Y. Sun, Y. Wu, B. Mayers, B. Gates, Y. Yin, F. Kim, H. Yan, *Adv. Mater.* 15 (2003) 353.
- [3] Y.S. Zhao, H. Fu, A. Peng, Y. Ma, D. Xiao, J. Yao, *Adv. Mater.* 20 (2008) 2859.
- [4] R. Li, W. Hu, Y. Liu, D. Zhu, *Acc. Chem. Res.* 43 (2010) 529.
- [5] L. Zang, Y. Che, J.S. Moore, *Acc. Chem. Res.* 41 (2008) 1596.

- [6] V.K. Praveen, S.S. Babu, C. Vijayakumar, R. Varghese, A. Ajayaghosh, *Bull. Chem. Soc. J.* 81 (2008) 1196.
- [7] Y. Zhou, W.J. Liu, Y. Ma, H. Wang, L. Qi, Y. Cao, J. Wang, J. Pei, *J. Am. Chem. Soc.* 129 (2007) 12386.
- [8] E. Ahmed, A.L. Briseno, Y. Xia, S.A. Jenekhe, *J. Am. Chem. Soc.* 130 (2008) 1118.
- [9] X.F. Duan, Y. Huang, R. Agarwal, C.M. Lieber, *Nature* 421 (2003) 241.
- [10] C.J. Barrelet, A.B. Greytak, C.M. Lieber, *Nano Lett.* 4 (2004) 1981.
- [11] R. Agarwal, C.J. Barrelet, C.M. Lieber, *Nano Lett.* 5 (2005) 917.
- [12] D.J. Sirbully, M. Law, H.Q. Yan, P.D. Yang, *J. Phys. Chem. B* 109 (2005) 15190.
- [13] J.C. Johnson, H.-J. Choi, K.P. Knutsen, R.D. Schaller, P. Yang, R.J. Saykally, *Nat. Mater.* 1 (2002) 106.
- [14] J.C. Johnson, H. Yan, P. Yang, R.J. Saykally, *J. Phys. Chem. B* 107 (2003) 8816.
- [15] J.Y. Kim, F.E. Osterloh, *J. Am. Chem. Soc.* 127 (2005) 10152.
- [16] A. Pan, R. Liu, Q. Yang, Y. Zhu, G. Yang, B. Zou, K. Chen, *J. Phys. Chem. B* 109 (2005) 24268.
- [17] Y. Qi, J. Ding, M. Day, J. Jiang, C.L. Callender, *Chem. Mater.* 17 (2005) 676.
- [18] K. Takazawa, *Chem. Mater.* 19 (2007) 5293.
- [19] K. Takazawa, *J. Phys. Chem. C* 111 (2007) 8671.
- [20] D. O'Carroll, I. Lieberwirth, G. Redmond, *Nat. Nanotech.* 2 (2007) 180.
- [21] D. O'Carroll, I. Lieberwirth, G. Redmond, *Small* 3 (2007) 1178.
- [22] H. Yanagi, T. Morikawa, *Appl. Phys. Lett.* 75 (1999) 187.
- [23] H. Yanagi, T. Ohara, T. Morikawa, *Adv. Mater.* 13 (2001) 1452.
- [24] F. Balzer, V.G. Bordo, A.C. Simonsen, H.-G. Rubahn, *Phys. Rev. B* 67 (2003) 115408.
- [25] K. Takazawa, Y. Kitahama, Y. Kimura, G. Kido, *Nano Lett.* 5 (2005) 1293.
- [26] A.N. Lebedenko, G.Y. Guralchuk, A.V. Sorokin, S.L. Yefimova, Y.V. Malyyukin, *J. Phys. Chem. B* 110 (2006) 17772.
- [27] S. Kanazawa, M. Ichikawa, T. Koyama, Y. Taniguchi, *ChemPhysChem* 7 (2006) 1881.
- [28] Y.S. Zhao, A. Peng, H. Fu, Y. Ma, J. Yao, *Adv. Mater.* 20 (2008) 1661.
- [29] Y.S. Zhao, J. Xu, A. Peng, H. Fu, Y. Ma, L. Jiang, J. Yao, *Angew. Chem. Int. Ed.* 47 (2008) 7301.

[30] Q. Liao, H. Fu, J. Yao, *Adv. Mater.* 21 (2009) 4153.

[31] H.B. Chen, Y. Zhou, J. Yin, J. Yan, Y. Ma, L. Wang, Y. Cao, J. Wang, J. Pei, *Langmuir* 25 (2009) 5459.

[32] F. Garca, F. Aparicio, M. Marenchino, R. Campos-Olivas, L. Sanchez, *Org. Lett.* 19 (2010) 4264.